Wet/dry etching combined microtextured structures for high-efficiency solar cells

Chan Seob Cho[1], *DaeYoung Kong*[1], *Bonghwan Kim*[2]

[1]*School of Electronic Engineering, Kyungpook National University, Daegu 702-701, Republic of Korea*
[2]*Department of Electronic and Electrical Engineering, Catholic University of Daegu, Gyeongbuk 712-702, Republic of Korea*
E-mail: bonghwan@gmail.com

Published in Micro & Nano Letters; Received on 28th May 2015; Accepted on 3rd August 2015

A solar cell texturing process using a two-step process that includes wet etching and dry etching has been developed. The surface reflectance and fill factor (FF) of the pyramid structure by general wet etching texturing process were 5.834 and 70.597%, respectively; the surface reflectance and FF of the two-step pyramid structure by wet etching and dry etching texturing process were 3.69 and 65.013%; and the surface reflectance and FF of the two-step pyramid structure by rounded pyramid and dry etching texturing process were 4.533 and 70.727%. The process of the two-step pyramid structure is as follows. First, the pyramid structure formed by the wet etching process was etched again with tetramethylammonium hydroxide solution. Then, the crest and the trough of the pyramid structure was fine etched, and rounded pyramid structures with a uniform n+ layer was formed. Secondly, a pyramid structure with a high angle on the rounded pyramid structure was formed by using reactive-ion etching with a metal mesh. The two-step pyramid structure by the wet etching and dry etching texturing process has a lower surface reflectance and higher FF than the pyramid structure formed of the wet etching texturing process. Therefore, the etching process is suitable for producing high-efficiency solar cells.

1. Introduction: The surface texturing process is a significant process in the production of crystalline silicon solar cells. A textured surface reduces light reflection of the front surface, increases the path length of the entered light and lowers wavelengths by an oblique trajectory between the cells of light absorption closer to the junction. Surface structures of low reflectivity are formed to increase the short-circuit current of a solar cell. The number of reflections of the incident light on the solar cell surface increases as the angle of the surface pyramid structure increases. Therefore, the light incident on the the solar cell can be increased [1–4].

The wet etching texturing process has a structural limitation with a pyramid angle of 54.74° due to the anisotropic etching characteristic of the single crystalline silicon. Therefore, the dry etching texturing process to form the pyramidal structure of a higher angle has been developed by many researchers. However, each pyramid structure with a high angle alone cannot produce high-efficiency solar cells [5–8].

For the production of solar cells to form a p–n junction, a pyramid structure formed by wet or dry etching process is doped as a non-uniform n+ layer. The non-uniform n+ layer is passed through a partial front electrode material at the firing process. As a result, the short-circuit current and open-circuit voltage of the solar cell is reduced by increasing the leakage current, and the fill factor (FF) of the solar cell is reduced by decreasing the shunt resistance. Therefore, it causes a decrease in the efficiency of solar cells.

The production of general crystalline silicon solar cells is achieved by first etching the cut and damaged part of the wafer using a silicon wet etching solution, then creating an uneven surface by a texturing process so as to decrease the surface reflectivity and then by increasing the absorbance of solar light. After formation of the emitter and deposition of antireflection coating through the doping process, a metal paste is used for the frontal and rear area of the wafer for screen printing, which creates electrodes. Lastly, contacting the created electrode with the emitter through the firing process at high temperatures results in the production of general crystalline silicon solar cells. In the current solar cell market, where the thickness of the substrate is gradually getting thinner and the kind of the substrate is becoming diverse, the texturing process done by wet etching is at its limit to meet the market requirements. It is an especially important process in determining the amount of incident light, but it cannot overcome its structural limits of holding a 54.74° pyramid angle due to the anisotropic etching nature of single crystalline silicon. As the pyramid angle increases, the number of beams of incident light reflected on the solar cell surface increases. This in turn increases the amount of incident light into the solar cell. Fig. 1 shows a schematic diagram of the wet saw damage removal (SDR) process and reactive-ion etching (RIE) texturing process with an additional wet etching process to improve the surface texturing structure. A general pyramid structure or spiked structure is formed on the surface with non-uniform thickness during processes such as the n+ doping process or the surface antireflection coat creation process of the solar cell production process [9–12]. The non-uniform n+ layer and the antireflection coat layer formed through the above process cannot generate the contact between the electrode and the n+ layer simultaneously on the whole area of the solar cell, but only generate sequential contact during the firing process which produces the upper electrode. The upper electrode that sequentially contacts the n+ layer forms an incomplete contact in which it passes the n+ layer, contacts within the n+ layer, but is unable to reach the n+ layer. Solar cells produced through the above process causes low parallel resistance, high J_0 and a low curve factor, which results in low efficiency. Therefore, through the firing process in solar cell production it is very difficult to form a stable processing condition [13, 14].

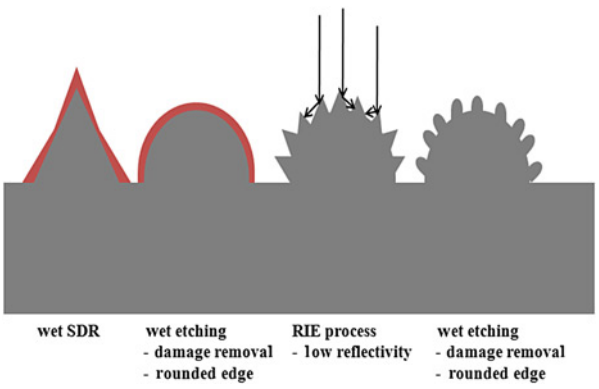

Fig. 1 *Schematic diagram of additional wet etching process and RIE texturing process*

doi: 10.1049/mnl.2015.0182

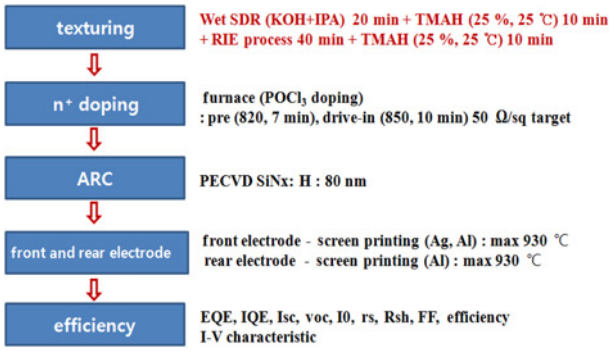

Fig. 2 *Solar cell fabrication flowchart*

Moreover, the RIE texturing process from former research allowed the acquisition of low surface reflectivity and high short-circuit current density but decreased the lifetime of the surface minority carrier due to RIE process damage and the degeneration of series resistance and parallel resistance due to fact that the uneven process (n+ layer and antireflection coat formation) could not bring about sufficient synergistic effect [15].

To minimise the decreasing effect occurring after the RIE process and to improve the spiked surface structure which is an ingrained problem of the texturing structure, the tetramethylammonium hydroxide (TMAH) anisotropic etching process was added. Fig. 1 shows the improved surface texturing structure formed through the repetition of the wet SDR process, the TMAH etching process and the RIE process. The texturing structure is a structure to lower the surface reflectivity by increasing the incidence angle of the incident light so that multiple reflections on the surface occur. Unfortunately the pyramid structure or the spiked structure formed to maintain a high incident angle causes the problems introduced above, so an appropriate compromise is needed. In this research, we investigated the improvement of surface reflectance and FF when the four different processing procedures were used: the wet SDR process is carried out to form a pyramid structure, then the corners are removed by the TMAH etching process, then fine uneven structures are formed through another etching of the RIE process and then the damage caused by the RIE process is eliminated by the TMAH process.

2. Experimental: Fig. 2 shows the flowchart of the solar cell fabrication. The substrate used in this research is p-type, with a resistivity 0.5–3 Ω cm, thickness 200 µm, with a 156 × 156 mm^2 (100), monocrystalline silicon wafer. The solar cells from the wet SDR process only to wet SDR + TMAH + RIE + TMAH process has been produced in each stage. The enhancement of solar cell quality by improving the texturing structure has been identified through the solar cells produced above. The n+ formation process, antireflection coat process and the upper and lower electrode formation process of the solar cell production process were carried out at the Southwestern Research Institute of Green Energy Technology to maintain the same conditions as the former research.

3. Results and discussion

3.1. Surface analysis: Fig. 3 shows the SEM result of the surface structure of each process. The surface is obtained by use of a potassium hydroxide (KOH, 45%) + isopropyl alcohol + deionised mixed solution to remove saw damage (SDR) for 20 min. After the SDR process, TMAH (25%) solution is used to improve the surface structure, the RIE process to decrease surface reflectivity and lastly the TMAH (25%, 25°C) etching process for 10 min to remove RIE damage. After the first wet SDR process, a sharp pyramid structure is formed on the surface. In the former research that used the RIE process to decrease surface reflectivity, 40 min

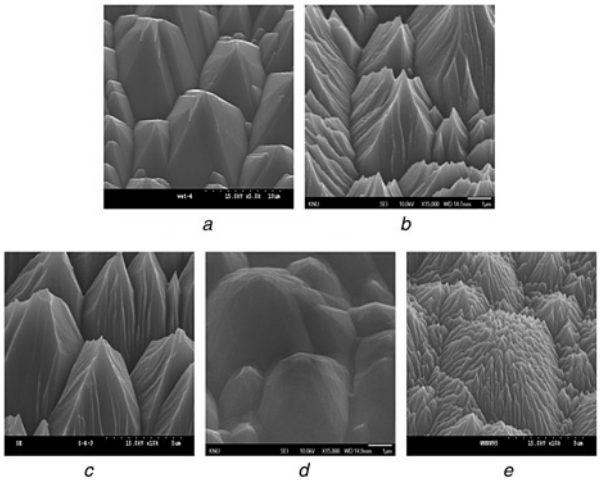

Fig. 3 *Surface of the solar cell substrate according to the texturing process*
a Wet SDR
b Wet SDR + RIE
c Wet SDR + RIE + TMAH
d Wet SDR + TMAH
e Wet SDR + TMAH + RIE + TMAH

processing allowed a valley-shaped unevenness on the surface with lower reflectivity and higher efficiency.

Therefore, in this research, the RIE process is performed for only 40 min. After the damage, which is formed by the RIE etching process and the TMAH wet etching process, is removed, valley-shaped pyramid structures are formed. By performing TMAH anisotropic etching after the wet SDR process, the sharp edges on the surface are removed, forming a surface structure similar to a hemisphere. The surface reflectivity of this structure increases, but it is thought to form a more uniform thickness after the n+ layer and antireflection coat formation process than that in the previous attempts.

The RIE process for 40 min on this structure creates a cactus-like small pyramid structure above the hemisphere structure, unlike the previously produced structure from RIE processing. Lastly, the TMAH process for 10 min will allow a final surface structure formed by the wet SDR + TMAH + RIE + TMAH texturing process as shown in the Figure. Surface reflectivity was the highest on the surface with only the wet SDR process (Fig. 4).

The surface structure similar to a hemisphere, formed by the wet SDR and TMAH process was expected to have the highest reflectivity, but it is thought that the space between the pyramidal structures formed previously were deeply etched after TMAH processing, resulting in a rather lower reflectivity. The surface reflectivity of the solar cell produced from wet SDR + TMAH +

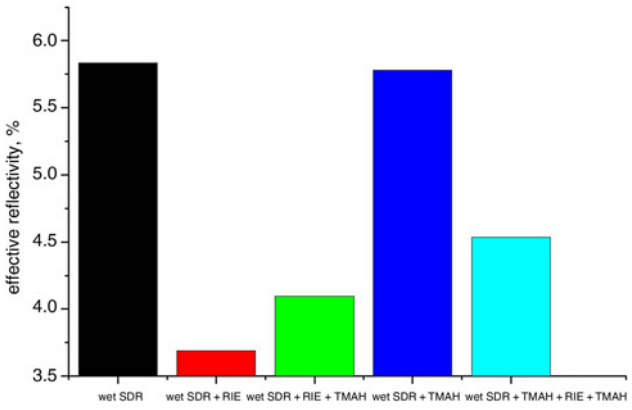

Fig. 4 *Effective reflectivity according to the texturing process*

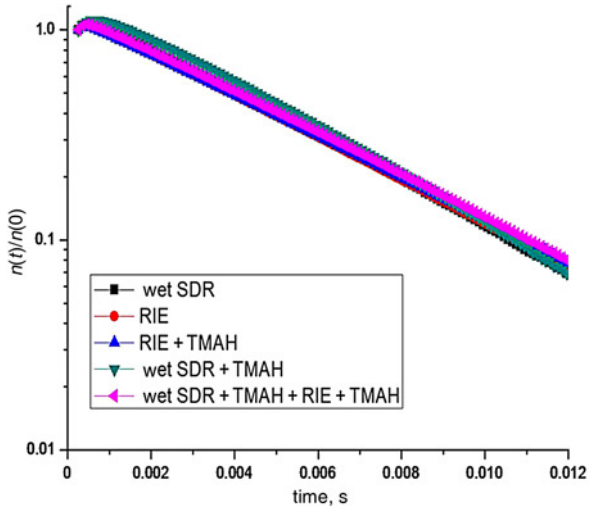

Fig. 5 *Graph of n(t)/n(0) against time*

RIE + TMAH texturing processing was also lower than the reflectivity of the solar cell produced from only the wet SDR process, allowing the short-circuit current density to increase and creating a structure that is able to improve the curve factor. The intensity of sunlight has a different value depending on its wavelength so it cannot be explained by the general average reflectivity value. Therefore, effective reflectivity was applied. The effective reflectivity in wet SDR, wet SDR + RIE, wet SDR + RIE + TMAH, wet SDR + TMAH and wet SDR + TMAH + RIE + TMAH were 5.834, 3.690, 4.095, 5.781 and 4.533%, respectively.

The wet SDR process had the highest effective reflectivity, followed by the wet SDR + TMAH processed surface and the wet SDR + TMAH + RIE + TMAH texturing processed solar cell. The solar cell produced from the wet SDR + RIE texturing process had the lowest effective reflectivity. The surface reflectivity were all after the antireflection coat was formed, so the difference in structural reflectivity largely decreased. However, it is expected that the solar cells with additional texturing processes will have a higher short-circuit current density than those with only the wet SDR process.

3.2. Quasi-steady-state photoconductance: Fig. 5 shows a graph of $n(t)/n(0)$ against time and minority carrier density against time after measurement of Quassi-Steady-State Photoconductance (QSSPC) in order to measure the minority carrier lifespan. The minority carrier lifetime can be obtained from the against time graph. The minority carrier lifetime of a solar cell with only the wet SDR process was 17.78 μs and the minority carrier lifetime of a solar cell with 40 min of RIE texturing process was 16.16 μs. The minority carrier lifetime of a solar cell with 40 min of RIE texturing process and additional TMAH process was 17.41 μs and the minority carrier lifetime of a solar cell with wet SDR process and additional TMAH process was 18.46 μs. Lastly, the minority carrier lifetime of a solar cell with the wet SDR + TMAH + RIE + TMAH texturing process was 18.73 μs.

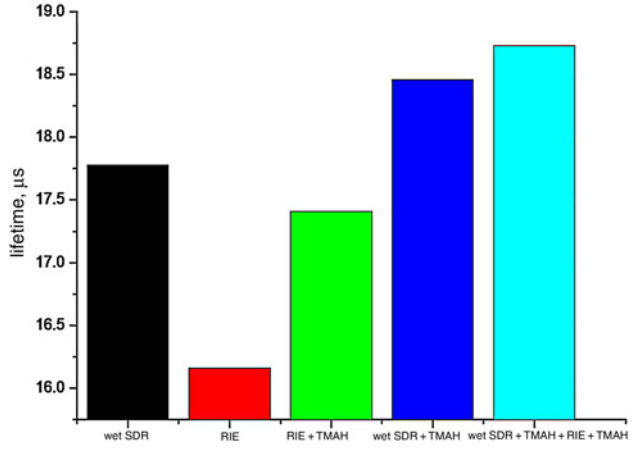

Fig. 6 *Lifetime*

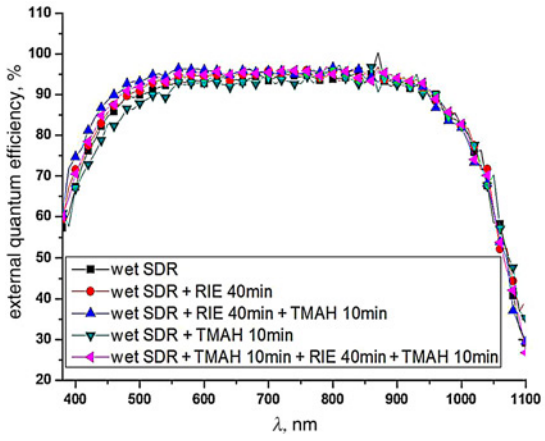

Fig. 7 *External quantum efficiency of solar cell*

Fig. 6 shows a schematic graph of minority carrier lifetime depending on the surface processing condition. It can be identified that after the RIE texturing process, the minority carrier lifetime decreases due to the plasma damage formed on the surface, and this could be removed through the TMAH etching process.

3.3. Quantum efficiency: Fig. 7 shows a graph of the external quantum efficiency of the solar cell depending on sunlight intensity at air mass (AM) 1.5. The quantum efficiency of the RIE + TMAH texturing processed solar cell was the highest in the short wavelength band, and the quantum efficiency of the wet SDR + TMAH texturing processed solar cell was the lowest in the short wavelength band.

3.4. Analysis of the quality of RIE texturing processed silicon solar cell: Fig. 8 is a graph of the current density–voltage characteristic of a solar cell during light irradiation. It can be identified from the Figure that the RIE texturing processed solar cell has high performance due to low reflectivity. As shown in the Figure, the surface structure exists in several various forms, but there is not

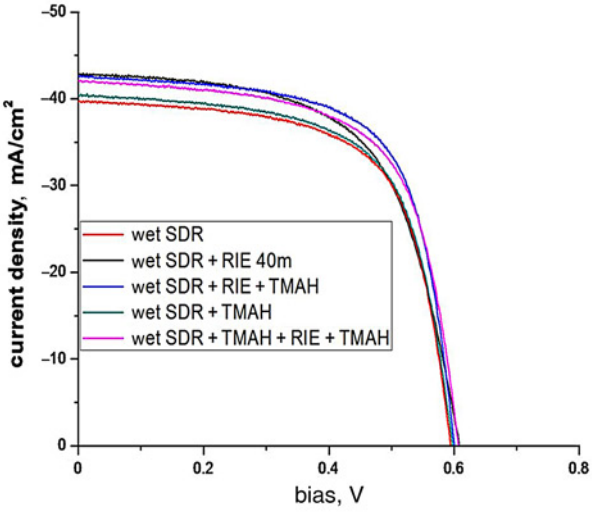

Fig. 8 *Current density–voltage characteristic of solar cell in the light*

doi: 10.1049/mnl.2015.0182

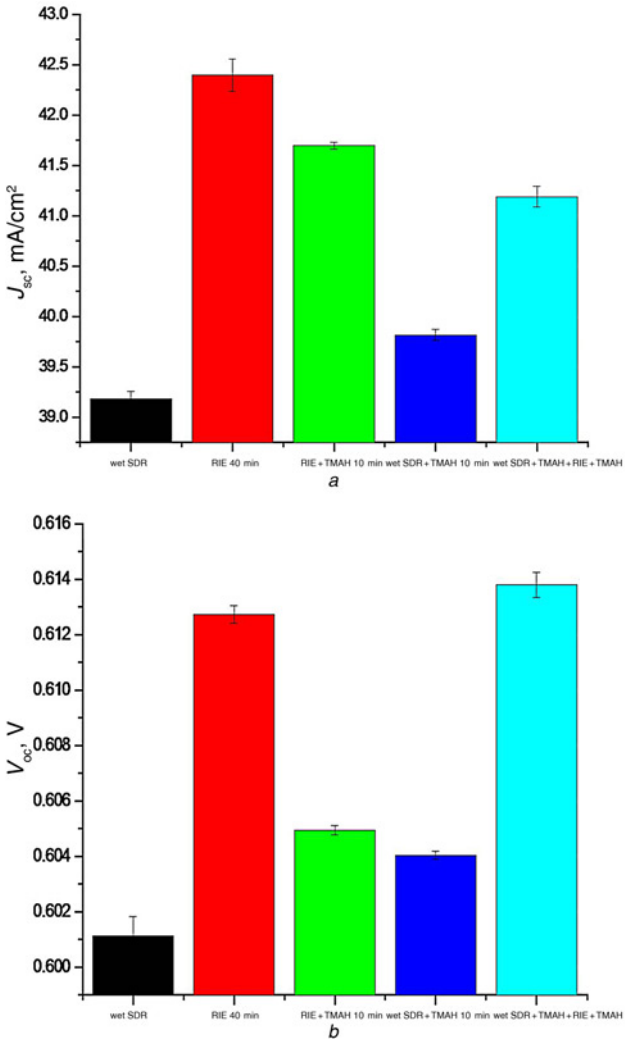

Fig. 9 *Solar cell processed*
a Short-circuit current density of solar cell
b Open-circuit voltage of solar cell

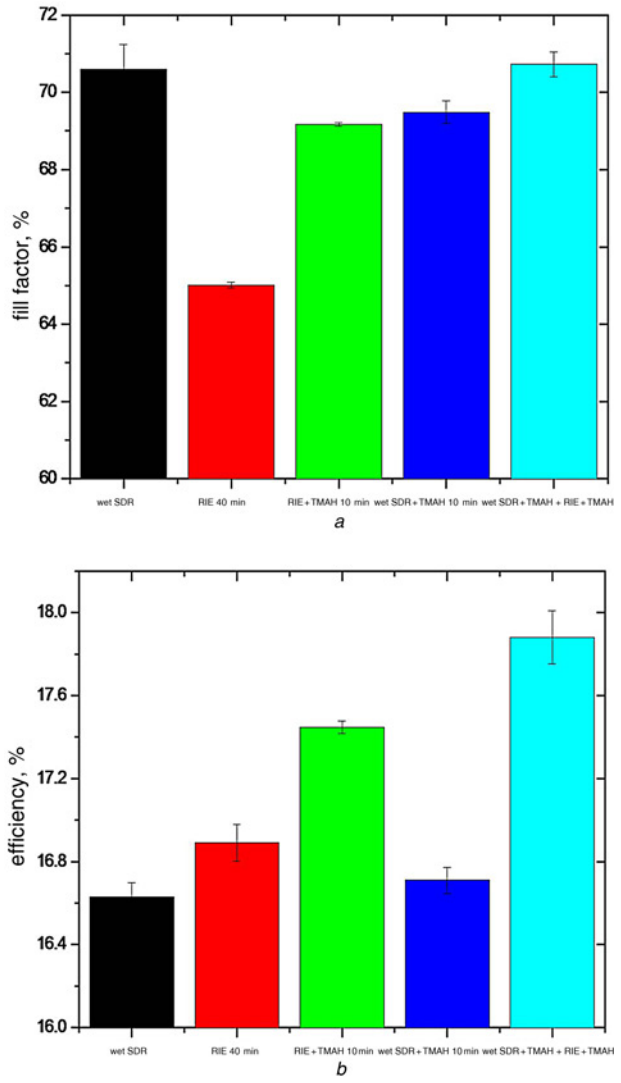

Fig. 10 *Curve factor of each solar cell and efficiency*
a FF of solar cell
b Efficiency of solar cell

much difference in open-circuit voltage. This is because short-circuit current density is closely related to the surface structure, but the open-circuit voltage is determined by the doping concentration and surface defect.

Fig. 9*a* shows the short-circuit current density of each solar cell. The short-circuit current density of the solar cell processed by wet SDR, RIE, RIE + TMAH, wet SDR + TMAH and wet SDR + TMAH + RIE + TMAH texturing were 39.18, 42.397, 41.697, 39.817 and 41.19 mA/m^2, respectively. The addition of the TMAH process after the RIE process improved the minority carrier lifetime, but the effect of surface reflectivity increase was greater so the short-circuit current density decreased. The TMAH process after the wet SDR process improved minority carrier lifetime as well as decreased surface reflectivity, which in turn increased short-circuit current density. The solar cell processed by wet SDR + TMAH + RIE + TMAH texturing appeared to have the highest open-circuit voltage (Fig. 9*b*). The open-circuit voltage for solar cells processed by wet SDR, RIE, RIE + TMAH, wet SDR + TMAH and wet SDR + TMAH + RIE + TMAH texturing were 0.601, 0.613, 0.605, 0.604 and 0.614 V, respectively. Fig. 10*a* shows the curve factor of each solar cell. The curve factor of solar cells processed by wet SDR, RIE, RIE + TMAH, wet SDR + TMAH and wet SDR + TMAH + RIE + TMAH texturing were 70.597, 65.013, 69.17, 69.49 and 70.727%, respectively.

The solar cell processed by RIE had a very big series resistance so its curve factor was much lower than other solar cells. The

Table 1 J_{sc}, V_{oc}, R_s, R_{sh}, J_0, FF, efficiency of solar cell comparison

	J_{sc}, mA/cm^2	V_{oc}, V	R_s, Ω	J_{sh}, Ω	J_0, A	FF, %	Efficiency, %
wet SDR	39.18	0.601	1.24	18.137	2.89×10^{-12}	70.597	16.63
RIE	42.397	0.613	2.667	26.891	3.34×10^{-12}	65.013	16.89
RIE + TMAH	41.697	0.605	1.59	21.198	3.13×10^{-12}	69.17	17.447
wet SDR + TMAH	39.817	0.604	1.37	16.946	2.72×10^{-12}	69.49	16.71
wet SDR + TMAH + RIE + TMAH	41.19	0.614	1.33	16.044	2.02×10^{-12}	70.727	17.88

TMAH process after the wet SDR process had a decrease in parallel resistance, so its curve factor decreased as well. The TMAH process after the RIE process had a decrease in parallel resistance, but had improved series resistance and so the open-circuit voltage increased, resulting in an increase in the curve factor. Fig. 10*b* shows the conversion efficiency of each solar cell. The conversion efficiency of the solar cells processed by wet SDR, RIE, RIE + TMAH, wet SDR + TMAH and wet SDR + TMAH + RIE + TMAH texturing was 16.63, 16.89, 17.447, 16.71 and 17.88%, respectively. The above results are organised in detail in Table 1. The results of this research were as expected, which allowed the wet SDR processed surface to have an improved curve factor by usage of TMAH, and decreased the surface reflectivity by the RIE process to increase the short-circuit current density.

4. Conclusion: In this research, the pyramidal and spiked structure on the surface formed by the wet SDR process or the RIE process was further etched by TMAH anisotropic etching solution; the edges of the pyramidal and spiked structure are removed and the texturing structure is improved, producing a surface structure of a solar cell with a high open-circuit voltage and curve factor. The short-circuit current density of the actual produced solar cell was increased by the RIE process and the minority carrier lifetime was enhanced by the TMAH process which in turn supplemented the surface texturing structure formed by the RIE process. The conversion efficiency of the produced solar cells was 16.63% for the wet SDR processed solar cell and 16.89% for the 40 min RIE processed solar cell. The conversion efficiency of the wet SDR + TMAH processed solar cell was 16.71% and the conversion efficiency of the RIE + TMAH processed solar cell was 17.447%. The surface texturing structure enhancement by TMAH etching after lowering the surface reflectivity by the RIE process had a more noticeable effect than the enhancement of the wet SDR processed solar cell. In conclusion, the solar cell processed by wet SDR + TMAH + RIE + TMAH had a very high efficiency of 17.88%. This is a 1.25% increase compared to the solar cell processed by wet SDR.

5. Acknowledgments: This research was supported by the Basic Science Research Program through the National Research Foundation of Korea (NRF) funded by the Ministry of Education (2013R1A1A4A01012255).

6 References

[1] Vazsonyi E., De Clercq K., Einhaus R., *ET AL.*: 'Improved anisotropic etching process for industrial texturing of silicon solar cells', *Sol. Energy Mater. Sol. Cells*, 1999, **57**, pp. 179–188

[2] Iencinella D., Centurioni E., Rizzoli R., *ET AL.*: 'An optimized texturing process for silicon solar cell substrates using TMAH', *Sol. Energy Mater. Sol. Cells*, 2005, **87**, pp. 725–732

[3] Weiying O., Yao Z., Hailing L., *ET AL.*: 'Texturization of monocrystalline silicon solar cell in TMAH without the addition of surfactant', *J. Semiconductors*, 2010, **31**, (10), p. 106002

[4] Santbergen R., van Zolingen R.J.C.: 'The absorption factor of crystalline silicon PV cells: a numerical and experimental study', *Sol. Energy Mater. Sol. Cells*, 2008, **92**, pp. 432–444

[5] Manea E., Budianu E., Purica M., *ET AL.*: 'Silicon solar cells parameters optimization by adequate surface processing techniques', *Rom. J. Inf. Sci. Tech.*, 2008, **11**, (4), pp. 337–345

[6] Zaidi S.H., Ruby D.S., Gee J.M.: 'Characterization of random reactive ion etched-textured silicon solar cells', *IEEE Trans. Electron Devices*, 2001, **48**, (6), pp. 1200–1206

[7] Dekkers H.F.W., Duerinckx F., Szlufcik J., *ET AL.*: 'Silicon surface texturing by reactive ion etching', *OPTO – Electron. Rev.*, 2000, **8**, pp. 311–316

[8] Yoo J., Kim K., Thamilselvan M., *ET AL.*: 'RIE texturing optimization for thin c-Si solar cells in SF_6/O_2 plasma', *J. Phys. D, Appl. Phys.*, 2008, **41**, p. 125205

[9] Dixit P., Miao J.: 'Effect of SF_6 flow rate on the etched surface profile and bottom grass formation in deep reactive ion etching process', *J. Phys., Conf. Series*, 2006, **34**, pp. 577–582

[10] Burtsev A., Li X., Zeijl Y.H.W., *ET AL.*: 'An anisotropic U-shaped SF_6-based plasma silicon trench etching investigation', *Microelectron. Eng.*, 1998, **40**, pp. 85–97

[11] Blakers A.W., Green M.A.: '20% efficiency silicon solar cells', *J. Appl. Phys.*, 1986, **48** (3), pp. 215–217

[12] Lee K.S., Ha M.-H., Kim J.H., *ET AL.*: 'Damage-free reactive ion etch for high-efficiency large-area multi-crystalline silicon solar cells', *Sol. Energy Mater. Sol. Cells*, 2011, **95**, pp. 66–68

[13] Xia Y., Liu B., Liu J., *ET AL.*: 'A novel method to produce black silicon for solar cells', *Sol. Energy*, 2011, **85** (7), pp. 1574–1578

[14] Moreno M., Daineka D., Cabarrocas P.R.I.: 'Plasma texturing for silicon solar cells: from pyramids to inverted pyramids-like structures', *Sol. Energy Mater. Sol. Cells*, 2010, **94**, pp. 733–737

[15] Panek P., Drabczyk K., Focsa A., *ET AL.*: 'A comparative study of SiO_2 deposited by PECVD and thermal method as passivation for multicrystalline silicon solar cells', *Mater. Sci. Eng. B*, 2009, **165**, pp. 64–66

doi: 10.1049/mnl.2015.0182